Dead-time Voltage Error Correction with Parallel Disturbance Observers for High Performance *V/f* Control

Tetsuma Hoshino, Jun-ichi Itoh
Department of Electrical Engineering
Nagaoka University of Technology
Nagaoka, Japan

Takayuki Kaneko
Electronics Technology Laboratory
Fuji Electric Advanced Technology Co., Ltd.
Tokyo, Japan

***Abstract*—This paper proposes a dead-time compensation method with a parallel disturbance observer and a current controller in the d-q rotational frame for *V/f* control. The parallel disturbance observers consist of a fast response disturbance observer and a slow response disturbance observer to separate the back electromotive force (EMF) from the estimated disturbance voltage. As a result, the dead-time error voltage is corrected using the proposed method. The proposed method is validated based on the simulation and experimental results. This method can improve the current distortion to less than 1/9 that of the conventional method.**

Keywords-component; induction motor, V/f control, dead-time, disturbance observer

I. INTRODUCTION

Recently, inverter systems have been applied to adjustable speed drive systems with induction motors in various fields for the economic utilization of energy. The *V/f* (motor voltage/output frequency) control method for an induction motor is more suitable to general applications than a speed sensor-less vector control method, because the *V/f* controller is very simple, and robust for variation of the motor parameters.

All voltage source type inverters require dead-time, which causes output voltage errors and has a significant effect on the low-voltage output range, such as at low speed. Therefore, dead-time compensation techniques are very important to realize a low cost motor drive system. Thus many dead-time correction methods are proposed [1-6]. In particular the most popular voltage error compensation method is feed forward compensation of the output voltage command according to the direction of the load current. This is very simple; however, it does not work well for the low speed range, because of difficulties in detection of the load current polarity [7]. Moreover, the precise dead-time compensation method, which based on dead-time error voltage measured toward the load current value in off-line, has been proposed [8]. However, this method is also difficult to compensate the dead-time error voltage because the dead-time voltage error values is influenced by the temperature and dispersion of a switching device.

On the other hand, dead-time compensation methods using a disturbance observer have been previously proposed [9-10]. In these reports, the disturbance observer is used for the sensor-less vector control system of a permanents magnet motor in a rotational frame or a three-phase frame. However, *V/f* control of the induction motor is not considered.

The dead-time compensation methods using a disturbance observer have some advantages as shown in next.

- Easier parameter setting than the other method.
- Possible to compensate forward drop voltage of a switching device, simultaneously.
- Possible to compensation in on-line at all times.

This paper proposes a dead-time compensation method with a parallel disturbance observer and a current controller in the d-q rotational frame for *V/f* control. This work is aimed at providing a simple and robust control system instead of speed sensor-less vector control. The voltage error on the d- and q-axes current caused by the dead-time is suppressed by an auto current regulator (ACR) in the d-axis and the disturbance observers in the q-axis. The parallel disturbance observers consist of a fast response disturbance observer and a slow response disturbance observer to separate the back electromotive force (EMF) from the estimated disturbance voltage. As a result, the dead-time error voltage is corrected using the proposed method. The proposed method is validated based on the simulation and experimental results. This method can improve the current distortion to less than 1/9 that of the conventional method.

II. PRINCIPLES OF DISTURBANCE OBSERVERS FOR DEAD-TIME ERROR VOLTAGE CORRECTION

A. Problems of dead-time and conventional compensation

Fig. 1 shows behavior of the voltage error during the dead-time period. Switch off time, it is so called dead-time, is added to gate pulses of u_p and u_n in order to avoid the short circuit between an upper arm and a lower arm. To obtain dead-time period, the turned-on timing of the gate pulse u_p and u_n are delayed during T_d as shown in Fig. 1(b).

The voltage error during the dead-time depends on the direction of a flowing current. When the output current direction of the leg is positive which is defined from the leg to load, the current in the leg flows through the free wheeling diode (FWD) of the lower arm during the dead-time period. Thus, the output voltage is decreased by the dead-time period. On the other hands, when the output current direction is negative, the current in the leg flows through the FWD of the upper arm. Thus, the output voltage increases. The value of the voltage error depends on the dead-time period and dc-link voltage as shown in Fig. 1. Finally, the voltage error is decided by (1).

$$\Delta V = f_s V_{dc} T_d \cdot \mathrm{sign}(i_u) \tag{1}$$

where, f_s: switching frequency, V_{dc}: dc-link voltage, T_d: dead-time period, i_u: output current of the leg, sign(x):sign function. If x>0 then sign(x) =1, if x<0 then sign(x) =1, if x=0 then sign(x) =0.

It should be noted that the magnitude of the voltage error does not depends on the amplitude of the output voltage and the output current. Therefore, when the output voltage is small such as a low speed operation, the affect of the dead-time is strongly appeared because the ratio of the voltage error to the output voltage becomes large.

B. Dead-time correction method using disturbance observers

Fig. 2 shows the equivalent circuit, in which a secondary leakage inductance is converted to a primary side, of an induction motor on d-q rotating frame. This paper proposes a dead-time compensation method with a disturbance observer. The voltage error of the dead-time is estimated by the output current and the motor parameters. The relation between the motor voltage v_1 and current i_1 is obtained by (2).

$$\begin{bmatrix} v_{1d} \\ v_{1q} \\ 0 \\ 0 \end{bmatrix} = \begin{bmatrix} R_1 + pL_\sigma & -\omega_1 L_\sigma & p & -\omega_1 \\ \omega_1 L_\sigma & R_1 + pL_\sigma & \omega_1 & p \\ -R_2 & 0 & \frac{R_2}{L_m} + p & -\omega_1 + \omega_m \\ 0 & -R_2 & \omega_1 - \omega_m & \frac{R_2}{L_m} + p \end{bmatrix} \begin{bmatrix} i_{1d} \\ i_{1q} \\ \phi_{2d} \\ \phi_{2q} \end{bmatrix} \tag{2}$$

where, R_1 is the primary resistance, R_2 is the secondary resistance, p is differential operator $p = d/dt$, L_m is the magnetizing inductance, L_σ is the equivalent leakage inductance, ω_1 is the primary angular frequency, ω_m is the secondary angular frequency, i_{1d} is d-axis components of the primary current on the d-q frame, i_{1q} is q-axis components of the primary current on d-q frame, v_{1d} is d-axis components of the primary voltage, v_{1q} is q-axis components of the primary voltage, ϕ_{2d} is d-axis components of secondary flux, and ϕ_{2q} is q-axis components of secondary flux.

From equation (2), when the d-axis corresponds to the vector for the secondary flux ϕ_2 and the q-axis component ϕ_{2q} is equal to zero, the q-axis voltage v_{1q} is calculated using (3).

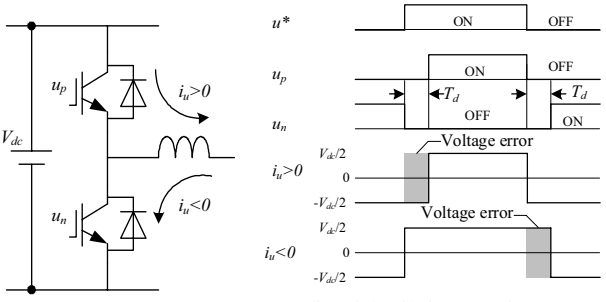

(a) An inverter leg. (b) Relationship between reference pulse and voltage error

Figure 1. Relations between reference pulse and voltage error.

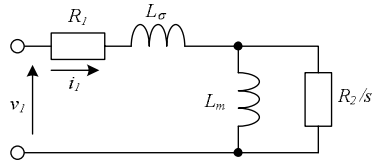

Figure 2. Equivalent circuit of induction motor.

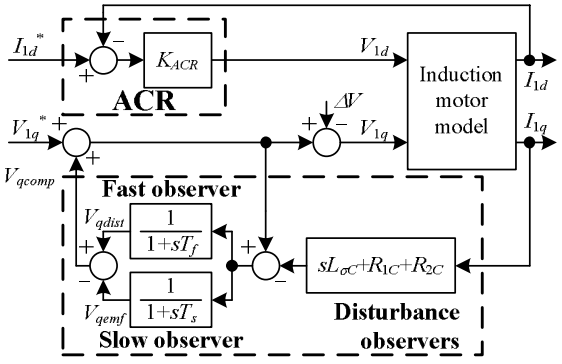

L_m: magnetizing inductance, ΔV: disturbance voltage, T_f, T_s: faster and slower time-constant of each disturbance observer, K_{ACR}: gain of the auto current regulator.

Figure 3. Block diagram of an induction-motor drive system using dead-time error correction using disturbance observers.

$$v_{1q} = (R_1 + R_2 + pL_\sigma) i_{1q} - \omega_1 L_\sigma i_{1d} + \omega_m \phi_{2d} . \tag{3}$$

In the equation (3), the 1st term of the right side change according to the electrical time constant $T_e = L_\sigma / (R_1+R_2)$ because the q-axis current respond at the electrical time constant. In contrast, the 3rd term of the right side changes slower than the 1st term, because the secondary angular frequency responds at the mechanical time constant. Then, the 2nd term means the cross-term.

The voltage error can be considered as the voltage disturbance for the q-axis current. In case of the low speed operation, ω_1 and ω_m in (3) become the small to other terms. Thus, if those small terms can be neglected, then the voltage error can be estimated using a voltage disturbance observer as shown in (4).

$$\Delta\hat{V} = \frac{1}{1+sT}\left(R_{1C} + R_{2C} + sL_{\sigma C}\right)I_{1q} \tag{4}$$

where, suffix $_C$ means controller parameter, T is time constant of the observer, s is Laplace operator, and I_{1q} is Laplace transfer of i_{1q}.

Fig. 3 shows a block diagram for the proposed compensation method using *V/f* control. The feedback filter using the T_f (fast response disturbance observer) estimates the back EMF in addition to the disturbance voltage. To estimate only the voltage error from dead-time in the middle- or high-speed range, the feedback filter of the T_s (slow response disturbance observer) is used to cancel the back EMF. On the other hand, the ACR on the d-axis corrects the dead-time voltage error on d-axis and maintains the rated excitation current of the motor.

III. Analyses of the Proposed System

One of advantages of a *V/f* control method is that a *V/f* control method is not sensitive for motor parameters in contrast to a speed sensor-less vector control. However the proposed voltage disturbance observers need some motor parameters. We are afraid that the proposed observer spoils the advantage of the conventional *V/f* method. Therefore, the parameter sensitivity of the proposed method is discussed based on transfer functions of the proposed system shown in Fig. 3, in this section.

A. Transfer functions of the proposed system

Before analysis of the proposed system, two low-pass filters written in connected in parallel, as shown in Fig. 3, is assembled as

$$G(s) = \frac{1}{1+sT_f} - \frac{1}{1+sT_s} = \frac{s\left(T_s - T_f\right)}{1+s\left(T_s + T_f\right)+s^2T_sT_f} \tag{5}.$$

From q-axis control part in Fig.3, the transfer functions to the output voltage V_{1q} from the voltage error ΔV or from the command voltage V_{1q}* in the Laplace plane are leaded as (6), (7).

$$\frac{V_q}{\Delta V} = \frac{1-G(s)}{1+G(s)\left(\frac{R_C}{R}\frac{1+sT_{eC}}{1+sT_e}-1\right)} \tag{6}$$

$$\frac{V_q}{V_q^*} = \frac{1}{1+G(s)\left(\frac{R_C}{R}\frac{1+sT_{eC}}{1+sT_e}-1\right)} \tag{7}$$

where R=R_1+R_2, R_C=R_{1C}+R_{2C}, $G(s)$ is the transfer function shown in (5)

B. Analyses of parameters mismatches using Bode diagrams

Fig. 4(a),(b) shows Bode diagrams for (6) and (7), respectively. The solid lines in Fig. 4 indicate an ideal condition, where $R_C = R$ and $L_{\sigma C} = L_\sigma$. In addition, the dashed lines indicate various conditions, where either R_C or $L_{\sigma C}$ is equal to R or L_σ multiplied or divided by ten. The other parameters used to calculate the Bode diagrams are given in Table. 1. In Fig. 4(a), lower magnitude indicates higher disturbance rejection performance. In Figure 4(b), 0 [dB] of magnitude means that controller outputs the same voltage to command voltage v_{1q}*.

Table 1. Analysis conditions.

Parameters	Values	Parameters	Values
Primary resistance R_1	2.78Ω	Fast response disturbance observer time constant T_f	1msec
Secondary resistance R_2	2.44Ω	Slow response disturbance observer time constant T_s	500msec
Leakage inductance L_σ	11.0mH		

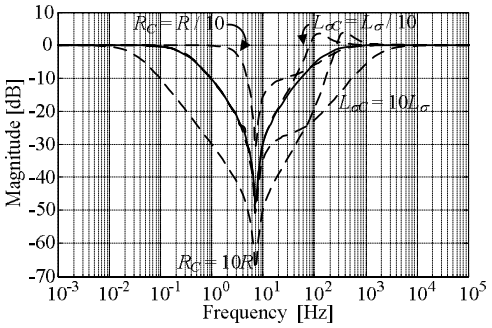

(a)Disturbance to output voltage transmission characteristics

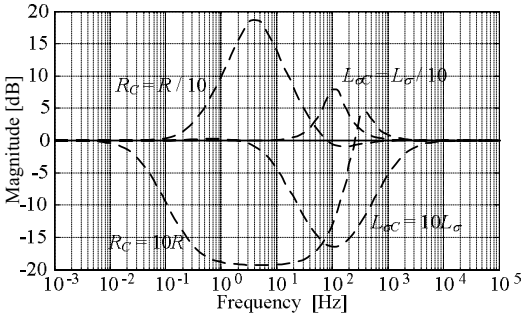

(b) Output voltage command to output voltage transmission characteristics

Figure 4. Frequency response of parallel connected disturbance observer system.

Then, parameter error sensitivities of each R_C and $L_{\sigma C}$ are considered.

1) Ideal conditon (R_C=R, $L_{\sigma C}$=L_σ)

Equation (8) is the transfer function from the voltage error ΔV to the output voltage V_{1q} based on (6) in case of the ideal condition in which the controller parameter agree with the motor parameter. It should be noted that the frequency response is same to a notch filters one at this ideal condition,. The center frequency of the notch is obtained by (9).

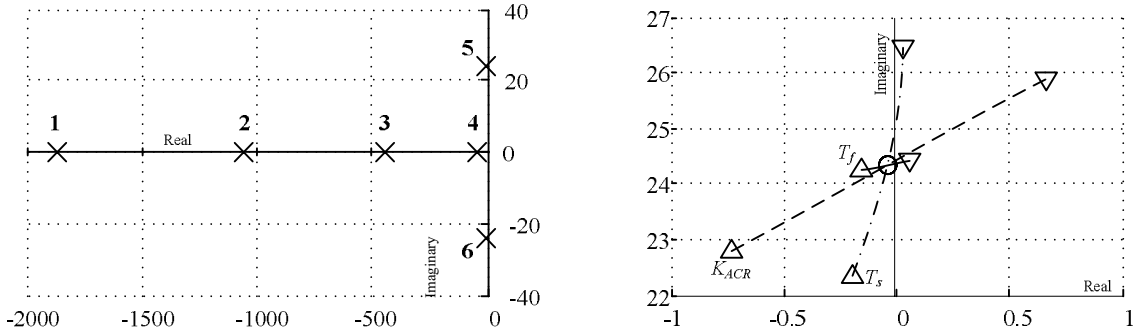

(a)Placement of six roots. (b) Trackings of the most vibratile root No.5.

Figure 5. Placement and tracking of roots. O indicates no parameter variations, Δ indicates +20%, and ∇ indicates –20%.
The solid line, dash-dot line and dashed lines represents the K_{ACR} current regulator gain, and the T_f and T_s observer time-constant variations, respectively.

$$\frac{V_q}{\Delta V} = \frac{1 + s(2T_f) + s^2 T_f T_s}{1 + s(T_f + T_s) + s^2 T_f T_s}. \quad (8)$$

$$f_0 = \frac{1}{2\pi\sqrt{T_s T_f}} \quad (9)$$

As a result, the disturbance rejection gain in Fig. 4(a) is 0 [dB] in a very low frequency region. It means that error voltage in the very low frequency region such as a low speed region can not be corrected. Therefore slow response disturbance observer time constant T_s have to be decided according to operation region of the system. Depending on the applications, the slow response disturbance observer may not use in the very low speed region.

2) Affection of the parameter R_C

In a middle and low frequency region, the disturbance voltage is suppressed by the proposed method, very well. Thus a speed control range of the system should be designed in this region. On the other hand, the performance of the disturbance voltage suppression is varied by the parameter R_C. If R_C is smaller than the R, then the performance will be worse. In contrast, if the R_C is bigger than the R, the performance will be better. Therefore, the control parameter R_C should be set to a little larger than the actual motor parameter R.

3) Affection of the parameter $L_{\sigma C}$

The affection of the parameter $L_{\sigma C}$ only appears in the high frequency region. However, the behavior is similar to the affection of the parameter R_C. That is, smaller $L_{\sigma C}$ improves the performance of the disturbance voltage suppression. In addition, bigger $L_{\sigma C}$ degrades the performance. Therefore, the control parameter $L_{\sigma C}$ should be set to a little smaller than the actual motor parameter L_σ. It should be note that the affection of the parameter $L_{\sigma C}$ is not too bigger than R.

Finally, we summarize the considerations about the parameter mismatch.

- The parameter mismatch of R affects considerably in the middle frequency region.
- The parameter mismatch of L_σ affects in the high frequency region.
- The gain of the controller from reference voltage V_{1q}* to output voltage V_{1q} is strongly affected by the parameter mismatch of R_C. The affection of the $L_{\sigma C}$ is smaller than affection of the R_C.

Therefore R_C must be determined with consideration for the error in R. However, the proposed system is not as sensitive as the speed sensor-less vector control system.

C. Stability analyses using roots trackings

The stability of the proposed system is analyzed using roots placement and tracking in the complex plane. The conditions for analyses use parameters of a general purpose 750 W induction motor under constant-speed in addition to those given in Table 1.

Fig. 5(a) shows the roots placement under the condition that T_f = 1 ms, T_s = 100 ms, K_{ACR} = 0.5 and $\omega_1 = \omega_m$ = 0.65 PU. This system has six roots because it is a sixth dimensional system. The placement of roots No.1-4 in Fig. 3 indicates sufficient stability, because those roots are dispersed on the real axis in an area that is negatively distant from the imaginary axis. However, the remaining roots, Nos. 5 and 6, are located nearest to the imaginary axis. Therefore, the stability of the proposed system can be discussed based on root No. 5.

Fig. 5(b) shows the root-No.5 trackings of variations in K_{ACR}, T_f, and T_s. Each of the parameters is varied ±20% from each of these values. To stabilize the system, the roots should be located in the area negatively distant from the imaginary axis, in addition to minimizing the imaginary part. Thus, T_f and T_s are set to slower values, and K_{ACR} is set to a higher value in order to realize stabilization of the system. It should be noted that a slow T_f avoids the error voltage correction, and a slow T_s deteriorates the acceleration performance due to the back EMF. In contrast, K_{ACR} should be set as high as possible for stabilization with the consideration about a delay time of the feedback loop. As a result, the parameters should be designed according to the next terms.

- T_f is set as faster as possible for controller.
- T_s is set to faster than the mechanical time-constant.
- After that, K_{ACR} is adjusted for the stability of the system.

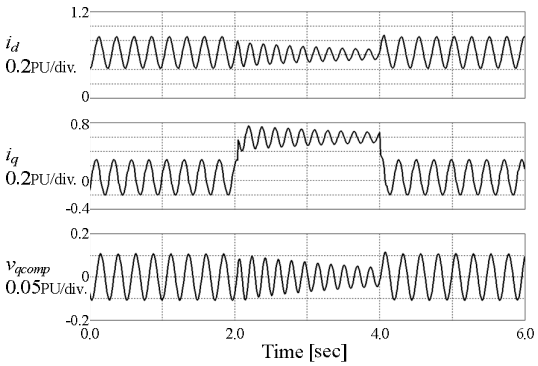

(a) D-axis ACR gain set to $K_{ACR} = 0.5$

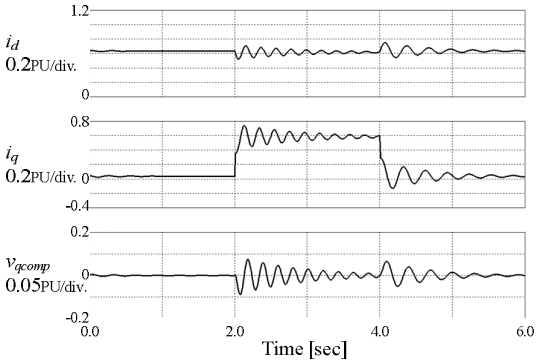

(b) D-axis ACR gain set to $2K_{ACR} = 1.0$

Figure 6. Damping result with parameter tuning.

Fig. 6 shows the d- and q-axis current, and the q-axis compensating voltage for verification of the stabilization with K_{ACR}. Each parameter has the same values as those used for the analyses except K_{ACR}. Note that the load condition is changed from no load to rated load at 2.0 sec, and from rated load to no load at 4.0 sec, as shown in Fig. 6. As shown in Fig. 6(a), the vibration in the current occurs because damping is not enough. In contrast, the vibration is converged by adjusting ACR gain K_{ACR} in Fig. 6(b). Therefore, the valid of the stabilization method is confirmed by the simulation.

IV. Experimental Result

Fig. 7 shows a control block diagram of an experimental system using the proposed *V/f* control. The experimental system is composed of a general induction motor and an inverter. The output voltage of the inverter is controlled on d and q rotating frame. The voltage command v_{1q}* is obtained on q-axis. In additions d-axis has the current regulator to maintain the exciting current and the stabilization.

Then, the proposed method is applied to the experimental system shown in Fig.7 so that the performance of the disturbance voltage rejection is inspected. Table 2 gives the experimental conditions of the controller and the motor. Note that slow response disturbance observer does not work in the low speed region according to the result in the section III-B.

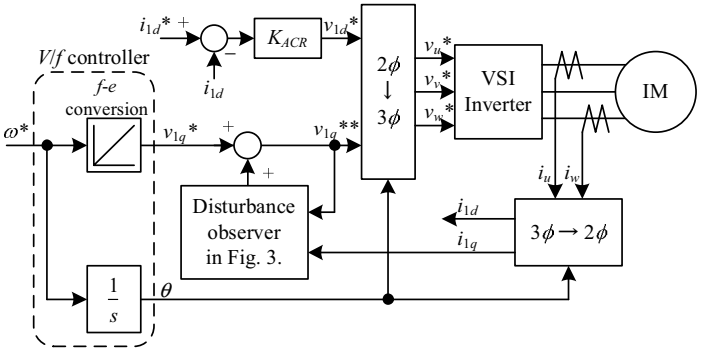

Figure 7. Experimental system.

Table 2. Experimental conditions.

Parameters	Values	Parameters	Values
Rated power	750W	Rated current	3.6A
Poles	4	Rated exciting current	2.0A
Rated voltage	200V	Primary resistance R_1	2.78Ω
Rated frequency	50Hz	Secondary resistance R_2	2.44Ω
Rated speed	1420r/min	Leakage inductance L_σ	11.0mH
Switching frequency	20kHz	Fast response disturbance observer time constant T_f	1msec
Dead-time period	3μsec	Slow response disturbance observer time constant T_s	10msec
D-axis ACR gain	2.0		

A. *Comparison of THD between the conventional method and the proposed method*

Fig. 8 shows the u-phase, d-axis and q-axis current waveforms under conditions where the output frequency is 1 Hz with no load. It should be noted that the conventional compensation method shown in Fig. 8(a) uses the voltage error feed-forward based on the current direction. The rated excitation current is maintained by the disturbance observers used in the proposed method as shown in Fig. 8(b). The total harmonic distortion (THD) of the current shown in Fig. 8(b) is 0.98%, with a 7.93 point reduction from the result as shown in Fig. 8(a).

Fig. 8(c) shows each harmonic components of u-phase current. The proposed method corrects the 2nd, 5th, and 7th harmonic component because of the decreasing of current stagnation at zero-crossing point.

B. *Comparison of steady state torque between the conventional method and the proposed method*

Fig. 9 shows the steady state torque curves. The output frequency is set to the rated slip of 2.67 Hz, and then decreases in speed. The starting torque (at 0 r/min) with the proposed method is 119%, which is six times the torque with the conventional method. Using the proposed method, the current stagnation at zero-crossing point of the conventional method is decreased, so that the current waveform is improved. It should be note that the torque curve of the proposed method exceeding the ideal line is caused by the over compensation for the voltage drop which depend on the primary resistance R_1.

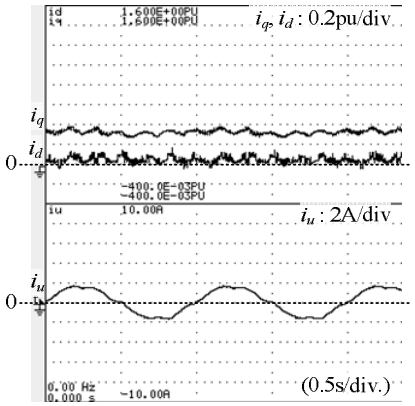

(a) Without proposed method

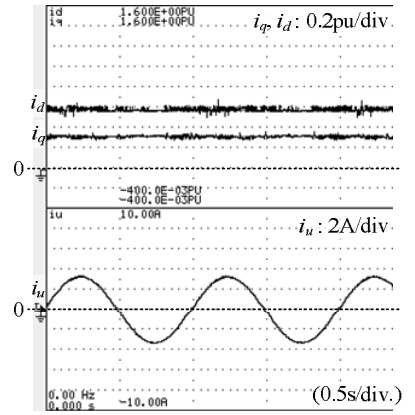

(b) With proposed method

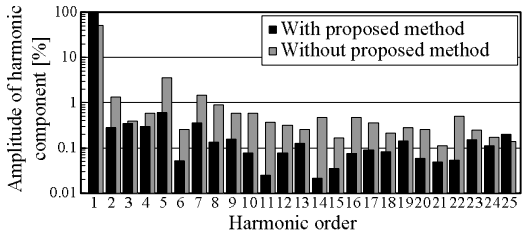

(c) Harmonic component in i_u waveform

Figure 8. Current waveforms at 1Hz under no-load condition.
(Output frequency 1Hz, no load, 750W induction motor)

C. *Dynamic state charactraistics*

Fig. 10 shows the characteristic responses to the step-shape load torque. The output frequency was set to 5 Hz, and the step load was applied at 1 sec. The proposed method works without stall against step-shape load, which means that the proposed method keeps stable in the dynamic state.

Fig. 11 shows the acceleration and braking characteristic between zero and the rated speed. The acceleration and braking time is set to 0.5 sec under the no load condition. The proposed method can generate high starting torque and acceleration torque though the middle and high speed region,

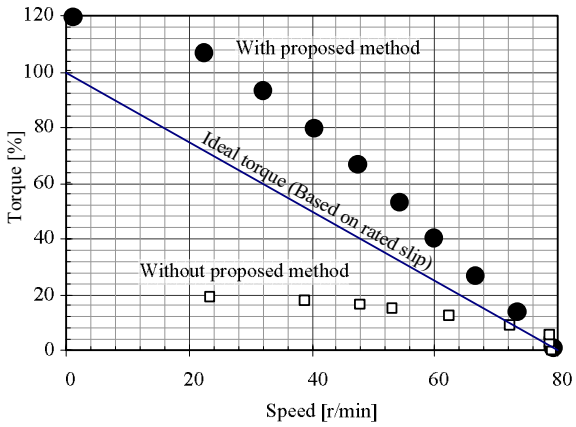

Figure 9. Improvement of steady state torque curve with proposed compensation method.

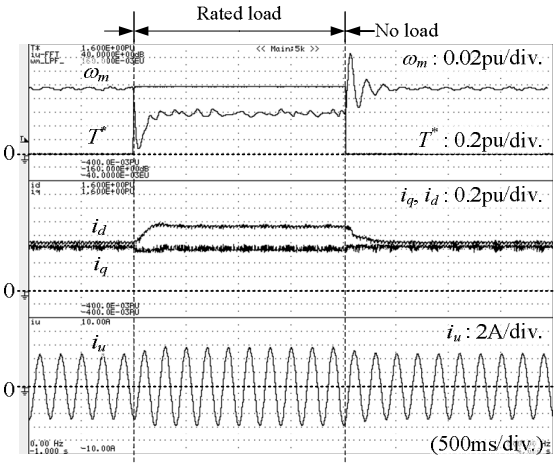

Figure 10. Characteristics against step-shape load torque.

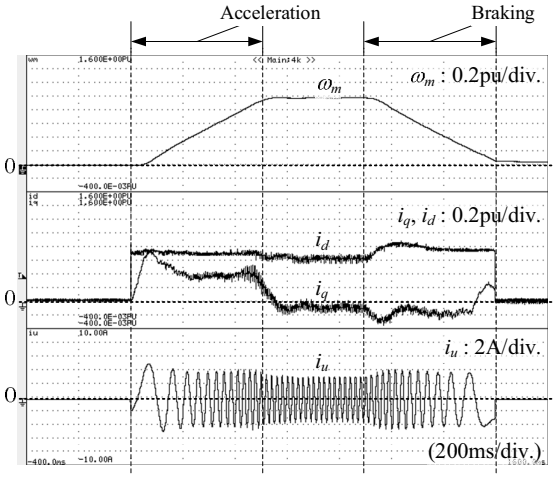

Figure 11. Characteristics against acceleration and braking.

because the slow response disturbance observer cancels back-EMF from the output of the fast response disturbance observer. In addition to acceleration, the proposed method can generate braking torque at all speed range.

D. *Verification of the affection of parameter mismatch*

Fig. 12 shows the affection of the THD by the variations of parameter mismatches of R_C or $L_{\sigma C}$.

When the R_C was smaller than the R, the THD is increased. Likewise, when the R_C was bigger than the R, the THD is decreased. On the other hands, when the parameter $L_{\sigma C}$ was different to the actual L_{σ}, the THD is increased. Those results agree with the conclusion in the section III-B. Thus, the validity of the analyses was confirmed.

V. CONCLUSIONS

A parallel disturbance observer, used for dead-time error voltage correction, was proposed and verified. A summary of the outcomes indicated in this study is as follows:

- The proposed method can suppress the disturbance voltage except back-EMF.
- The THD of the motor current is improved by less than 1/9 that for the conventional method.
- Using the proposed method, the starting torque is improved to 119%, which is six times that for the conventional method.
- The parameter mismatch does not causes significantly performance degradation.
- The proposed method is robust against the dynamic loads e.g. step load torque and acceleration.

ACKNOWLEDGMENT

This study was supported by Industrial Technology Grant Program in 2005 from New Energy and Industrial Technology Development Organization (NEDO) of Japan.

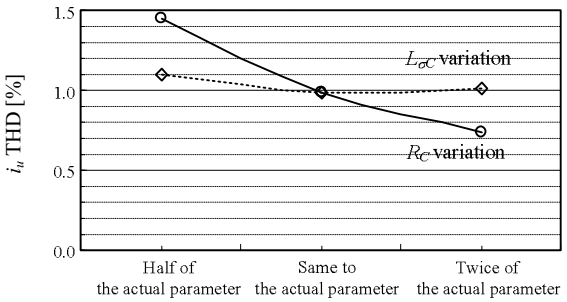

Figure 12. THD variations about parameter mismatching.

REFERENCES

[1] T. Sukegawa, K. Kamiyama, K. Mizuno, T. Matsui, and T. Okuyama, : "Fully digital vector-controlled PWM VSI fed ac drives with an inverter dead-time compensation strategy," IEEE Transaction on Industry. Application., vol. 27, no. 3, pp. 552–559, (May/Jun. 1991).

[2] J. W. Choi and S. K. Sul, : "Inverter output voltage synthesis using novel dead time compensation," IEEE Transaction on Power Electronics, vol. 11, no. 2, pp. 221–227, (Mar. 1996).

[3] A. R. Munoz and T. A. Lipo, : "On-line dead-time compensation technique for open-loop PWM-VSI drive," IEEE Transaction on Power Electronics , vol. 14, no. 4, pp. 683–689, (Jul. 1999).

[4] S.-G. Jeong and M.-H. Park, "The analysis and compensation of deadtime effects in PWM inverters," IEEE Transaction on Industry. Electronics., vol. 38, no. 2, pp. 108–114, Apr. 1991.

[5] A. Muñoz-Garcia and T. A. Lipo, "On-line dead-time compensation technique for open-loop PWM-VSI drive," IEEE Transaction on Power Electronics, vol. 14, no. 4, pp. 683–689, Jul. 1999.

[6] A. Cichowski, J. Nieznanski, "Self-Tuning Dead-Time Compensation Method for Voltage-Source Inverters" IEEE Power Electronics Letters, vol. 3, no. 2, June 2005

[7] H. Zhao, Q. M. J. Wu, and A. Kawamura, "An accurate approach of non-linearity compensation for VSI inverter output voltage," IEEE Transaction on Power Electronics., vol. 19, no. 4, pp. 1029–1035, Jul. 2004

[8] S. Kakizaki, M. Ito, T. Fukumoto, H. Hamane, and Y. Hayashi, "Measurment of Parameters and the Automatic Measurement of an Error Voltage by Dead Time of an Induction Motor" IEEJ Annual meeting, 4-143, (Mar. 2007)

[9] H. S. Kim, H. T. Moon, and M. J. Youn, : "On-line dead-time compensation method using disturbance observer," IEEE Transaction on Power. Electronics., vol. 18, no. 6, pp. 1136–1345, (Nov. 2003).

[10] N. Urasaki, T. Senjyu, K. Uezato, T. Funabashi, : "An Adaptive Dead-Time Compensation Strategy for Voltage Source Inverter Fed Motor Drives" IEEE Transactions on Power Electronics, Vol. 20, No. 5, (Sep. 2005).